Dinuclear tetrapyridyl pendant-armed azamacrocyclic complexes of Co(II), Ni(II), Cu(II) and Cd(II)

Mª del Carmen Fernández-Fernández [b], Rufina Bastida [b,*], Alejandro Macías [b],
Paulo Pérez-Lourido [a], Laura Valencia [a,*]

[a] Departamento de Química Inorgánica, Facultad de Química, Universidade de Vigo, As Lagoas, Marcosende, 36310 Vigo, (Pontevedra), Spain
[b] Departamento de Química Inorgánica, Facultad de Química, Universidad de Santiago de Compostela, Avenida de las Ciencias s/n, 15782 Santiago de Compostela (La Coruña), Spain

ARTICLE INFO

ABSTRACT

The coordination capability of the new tetrapyridyl pendant-armed azamacrocyclic ligand L, towards Co(II), Ni(II), Cu(II) and Cd(II) ions was studied. The ligand and the complexes were characterized by microanalysis, LSI mass spectrometry, IR, UV–Vis and NMR spectroscopy, magnetic studies and conductivity measurements. Crystal structures of $[Co_2L(CH_3CN)_2](ClO_4)_4 \cdot 2CH_3CN$ and $[Cd_2L(NO_3)_2](NO_3)_2 \cdot 2H_2O$ complexes have been determined. The X-ray studies show the presence of dinuclear endomacrocyclic complexes with the metal ion in a similar distorted octahedral environment, coordinated by one pyridyl bridgehead group, two amine nitrogen atoms and two pyridyl pendant-arms. The sixth coordination position around the metal ion is completed by one acetonitrile molecule in $[Co_2L(CH_3CN)_2](ClO_4)_4 \cdot 2CH_3CN$ and by one monodentate nitrate anion in $[Cd_2L(NO_3)_2](NO_3)_2 \cdot 2H_2O$. Different sort of intramolecular non-classical hydrogen bonds were found in the crystal lattice of both structures.

© 2009 Elsevier B.V. All rights reserved.

1. Introduction

Polyazamacrocyclic ligands have been a subject extensively investigated in the coordination chemistry research during last three decades due its ability to form complexes with different metal ions or anionic species with considerable potential in such areas as catalysis, modelling of metalloenzyme, molecular recognition, etc [1–5].

The presence of pendant-arms into the macrocyclic skeleton have attracted a great deal of interest owing to the fact that the ligating groups attached to the macrocyclic backbone can offer additional donor groups to produce important changes in the control of the stability, selectivity, stereochemistry and certain thermodynamic parameters [6–9], or promote the formation of dinuclear or polynuclear metal complexes with interaction between the metal centres, as well as act as hosts for organic cations with different properties and applications [1,4]. Several examples of macrocyclic ligands bearing pyridyl pendant groups have been described in the literature [10–12]. The flexibility of those pendant groups makes them a more versatile molecules, which allow coordination of the encapsulated metal or promotes

the formation of polymeric complexes, depending on the steric requirements of the metal ion employed [13,14].

In this sense, the ligand L^1 (Scheme 1) have resulted to be a sample of versatile pendant-armed azamacrocyclic ligand from which many metal complexes of different nuclearities and properties were prepared [15–19].

Hence, as part as our research in the macrocyclic coordination area, we have previously reported a metal complex series of the potential hexadentate azamacrocyclic ligand L' [20–22]. Now, we described here the synthesis and the structural characterization of a series of dinuclear complexes of Co(II), Ni(II), Cu(II) and Cd(II) with the tetrapyridyl hexaazamacrocycle L, obtained by attaching four pyridyl pendant groups to the macrocycle L'.

2. Experimental

2.1. Chemicals and starting materials

The macrocyclic precursor L' has been synthesized following the previously reported method [20]. 2,6-Diacetylpyridine, ethylendiamine, Ba(II) chloride, 2-picolyl chloride hydrochloride, $Co(NO_3)_2 \cdot 6H_2O$, $Ni(NO_3)_2 \cdot 6H_2O$, $Cu(NO_3)_2 \cdot 3H_2O$, $Cd(NO_3)_2 \cdot 4H_2O$, $Co(ClO_4)_2 \cdot 6H_2O$, $Ni(ClO_4)_2 \cdot 6H_2O$, $Cu(ClO_4)_2 \cdot 6H_2O$ and $Cd(ClO_4)_2 \cdot 6H_2O$ were commercial products obtained from Alfa and Aldrich, and were used without further purifications. The solvents used were of reagent grade and purified by usual methods.

* Corresponding authors. Tel.: +34 986 812607; fax: +34 986 813797 (L. Valencia), tel.: +34 981 591076; fax: +34 981597525 (R. Bastida).
E-mail addresses: qibastid@usc.es (R. Bastida), qilaura@uvigo.es (L. Valencia).
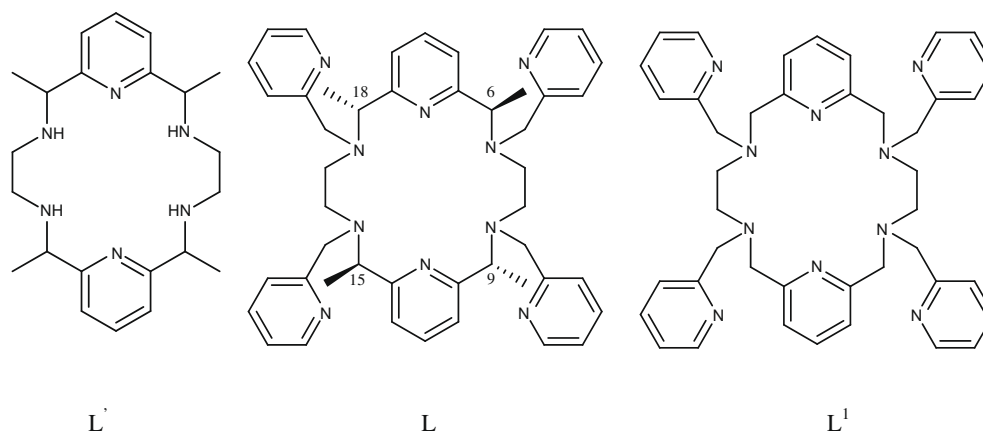
Scheme 1.

Caution: Although no problems were encountered during the course of this work, attention is drawn to the potentially explosive nature of perchlorate salts.

2.2. Synthesis of the macrocyclic ligand, L

The synthesis of the ligand L was achieved starting from the isomeric mixture of the macrocyclic precursor L′.

The precursor ligand L′ (3 mmol, 1.15 g) was dissolved in acetonitrile (100 mL) under reflux and 2-picolyl chloride hydrochloride (18 mmol, 2.95 g) and Na_2CO_3 (40 mmol, 4.32 g) were added. The mixture was refluxed for 6 h and stands to cool. The solution was filtered off and evaporated to dryness. The residue was then extracted with water–chloroform. The organic layer was dried over anhydrous Na_2SO_4 and evaporated to yield a brown oil that was recrystallised in acetonitrile giving the ligand L as a white solid.

Anal. Calc. for $C_{46}H_{54}N_{10}$ (MW: 747): C, 74.0; H, 7.3; N, 18.7. Found: C, 73.9; H, 7.3; N, 18.6%. Yield: 52%. IR (KBr, cm^{-1}): 1589, 1571, 1459, 1434 [$v(C=N)_{py}$ and $v(C=C)$]. LSI–MS, m/z: 748 [L+H]$^+$. Color: white.

2.3. Physical measurements

Elemental analyses were performed in a Carlo-Erba EA microanalyser. LSI–MS were recorded using a Micromass Autospec spectrometer with 3-nitrobenzyl alcohol as the matrix. Infra-red spectra were recorded as KBr discs on a Bruker IFS-66 V spectrophotometer. Solid state electronic spectra were recorded on a Hitachi 4-3200 spectrophotometer using $MgCO_3$ as reference. Magnetic studies were determined at room temperature on a vibration sample magnetometer (VSM) Digital Measurement System 1660 with a magnetic field of 5000 G. Conductivity measurements were carried out in 10^{-3} mol dm^{-3} acetonitrile solutions at 20 °C using a WTW LF3 conductivimeter. NMR spectra were recorded on a Bruker 500 MHz using CDCl$_3$ as solvent.

2.4. X-ray data collection, structure determination, and refinement

Slow recrystallization from acetonitrile gave crystals of [Co$_2$L(CH$_3$CN)$_2$](ClO$_4$)$_4$·2CH$_3$CN and [Cd$_2$L(NO$_3$)$_2$](NO$_3$)$_2$·2H$_2$O suitable for X-ray diffraction. The details of the X-ray crystal data, and the structure solution and refinement are given in Table 1. Measurements were made on a Bruker SMART CCD 1000 area diffractometer. All data were corrected for Lorentz and polarization effects. Empirical absorption corrections were also applied for all the crystal structures obtained [23]. Complex scattering factors were taken from the program package SHELXTL [24]. The structures were solved by direct methods which revealed the position of all

non-hydrogen atoms. All the structures were refined on F^2 by a full-matrix least-squares procedure using anisotropic displacement parameters for all non-hydrogen atoms. The hydrogen atoms were located in their calculated positions and refined using a riding model.

2.5. Synthesis of metal complexes – general procedure

The reactions were carried out in 1:1 metal:ligand molar ratio in all cases. The appropriate metal salt (0.5 mmol) was dissolved in acetonitrile (10 ml) and added to a stirred solution of the macrocyclic ligand L (0.5 mmol) in acetonitrile (15 ml). The solution was stirred for 3 h and concentrated to the air at room temperature to obtain crystalline precipitates The resulting products were filtered off, dried and recrystallized from acetonitrile.

2.5.1. [Co₂L](NO₃)₄

Anal. Calc. for $C_{46}H_{54}N_{14}O_{12}Co_2$ (MW: 1112.9): C, 49.6; H, 4.9; N, 17.6. Found: C, 49.5; H, 4.8; N, 17.4%. Yield: 37%. IR (KBr, cm^{-1}): 1606, 1577, 1444 [$v(C=N)_{py}$ and $v(C=C)$], 1384, 1058, 838, 767 [$v(NO_3^-)$]. LSI–MS, m/z: 989 [Co$_2$L(NO$_3$)$_3$]$^{2+}$, 927 [Co$_2$L(NO$_3$)]$^{3+}$, 865 [Co$_2$L]$^{4+}$. $\Lambda_M/\Omega^{-1}cm^2mol^{-1}$ (in CH$_3$CN): 210 (2:1). Color: pink.

2.5.2. [Co₂L](ClO₄)₄·4CH₃CN

Anal. Calc. for $C_{54}H_{66}N_{14}O_{16}Cl_4Co_2$ (MW: 1426.9): C, 45.5; H, 4.7; N, 13.7. Found: C, 45.7; H, 4.7; N, 13.6%. Yield: 35%. IR (KBr, cm^{-1}): 1606, 1575, 1444 [$v(C=N)_{py}$ and $v(C=C)$], 1091, 626 [$v(ClO_4^-)$]. LSI–MS, m/z: 865 [Co$_2$L]$^{4+}$. $\Lambda_M/\Omega^{-1}cm^2mol^{-1}$(in CH$_3$CN): 480 (4:1). Color: pink.

2.5.3. [Ni₂L](NO₃)₄·2H₂O

Anal. Calc. for $C_{46}H_{58}N_{14}O_{14}Ni_2$ (MW: 1092): C, 48.1; H, 5.1; N, 17.1. Found: C, 48.1; H, 5.3; N, 17.2%. Yield: 44%. IR (KBr, cm^{-1}): 1608, 1587, 1448 [$v(C=N)_{py}$ and $v(C=C)$], 1384, 1031, 831, 767 [$v(NO_3^-)$]. LSI–MS, m/z: 989 [Ni$_2$L(NO$_3$)$_3$]$^{2+}$, 927 [Ni$_2$L(NO$_3$)$_2$]$^{3+}$, 865 [Ni$_2$L]$^{4+}$. $\Lambda_M/\Omega^{-1}cm^2mol^{-1}$ (in CH$_3$CN): 258 (2:1). Colour: green.

2.5.4. [Ni₂L](ClO₄)₄·2CH₃CN

Anal. Calc. for $C_{50}H_{60}N_{12}O_{16}Cl_4Ni_2$ (MW: 1340.2): C, 44.8; H, 4.5; N, 12.5. Found: C, 44.7; H, 4.6; N, 12.3%. Yield: 50%. IR (KBr, cm^{-1}): 1608, 1582, 1448 [$v(C=N)_{py}$ and $v(C=C)$], 1091, 630 [$v(ClO_4^-)$]. LSI–MS, m/z: 862 [Ni$_2$L]$^{4+}$. $\Lambda_M/\Omega^{-1}cm^2mol^{-1}$(in CH$_3$CN): 447 (4:1). Colour: green.

2.5.5. [Cu₂L](NO₃)₄

Anal. Calc. for $C_{46}H_{54}N_{14}O_{12}Cu_2$ (MW: 1120.3): C, 49.3; H, 4.9; N, 17.5. Found: C, 48.7; H, 4.9; N, 17.4%. Yield: 42%. IR (KBr, cm^{-1}):

Table 1
Crystal data and structure refinement for [Co$_2$L(CH$_3$CN)$_2$](ClO$_4$)$_4$·2CH$_3$CN and [Cd$_2$L(NO$_3$)$_2$](NO$_3$)$_2$·2H$_2$O.

	Co$_2$L(CH$_3$CN)$_2$(ClO$_4$)$_4$.2CH$_3$CN	Cd$_2$L(NO$_3$)$_2$(NO$_3$)$_2$.2H$_2$O
Empirical formula	C$_{27}$H$_{33}$N$_7$O$_8$Cl$_2$Co	C$_{46}$H$_{58}$N$_{14}$O$_{14}$Cd$_2$
Formula weight	713.43	1255.86
Temperature (K)	293(2)	293(2)
Wavelength (Å)	0.71073	0.71073
Crystal system	Monoclinic	Monoclinic
Space group	P21/n	P21/n
Unit cell dimensions		
	a = 13.729(2) Å	*a* = 19.346(7) Å
	b = 13.572(2) Å	*b* = 13.279(5) Å
	β = 102.972(3)°	*β* = 104.956(6)°
	c = 16.986(3) Å	*c* = 20.608(8) Å
Volume (Å^3)	3084.4(8)	5115(3)
Z	4	4
Density (calculated) (Mg/m^3)	1.536	1.631
Absorption coefficient (mm^{-1})	0.790	0.911
F(0 0 0)	1476	2560
Crystal size	0.23 × 0.17 × 0.07 mm^3	0.24 × 0.22 × 0.10 mm^3
θ Range for data collection	1.94–26.02°	1.29–27.11°
Index ranges	−16 ⩽ h ⩽ 16, 0 ⩽ k ⩽ 16, 0 ⩽ l ⩽ 20	−24 ⩽ h ⩽ 23, 0 ⩽ k ⩽ 16, 0 ⩽ l ⩽ 26
Reflections collected	26438	46052
Independent reflections	6064 [*R*(int) = 0.0490]	11227 [*R*(int) = 0.0333]
Completeness to *θ*	99.9% (26.02°)	99.4% (27.11°)
Absorption correction	Sadabs	Sadabs
Maximum and minimum transmission	0.9468 and 0.8391	0.9144 and 0.8109
Refinement method	Full-matrix least-squares on F^2	Full-matrix least-squares on F^2
Data/restraints/parameters	6064/0/408	11227/0/689
Goodness-of-fit on (GOF) F^2	1.065	1.049
Final *R* indices [*I* > 2σ(*I*)]	R_1 = 0.0483, wR_2 = 0.1255	R_1 = 0.0400, wR_2 = 0.0956
R indices (all data)	R_1 = 0.0825, wR_2 = 0.1404	R_1 = 0.0657, wR_2 = 0.1063
Largest difference in peak and hole (e Å^{-3})	0.573 and −0.351	1.001 and −0.575

1608, 1588, 1444 [v(C=N)$_{py}$ and v(C=C)], 1384, 825, 765 [v(NO$_3^-$)]. LSI–MS, *m/z*: 996 [Cu$_2$L(NO$_3$)$_2$]$^{2+}$, 934 [Cu$_2$L(NO$_3$)]$^{3+}$, 872 [Cu$_2$L]$^{4+}$. Λ_M/Ω^{-1}cm^{2}mol^{-1} (in CH$_3$CN): 265 (2:1). Colour: blue.

2.5.6. [Cu$_2$L](ClO$_4$)$_4$·3CH$_3$CN

Anal. Calc. for C$_{52}$H$_{63}$N$_{13}$O$_{16}$Cl$_4$Cu$_2$ (MW: 1391.2): C, 44.8; H, 4.6; N, 13.1. Found: C, 45.1; H, 4.5; N, 12.9%. Yield: 46%. IR (KBr, cm^{-1}): 1608, 1477, 1444 [v(C=N)$_{py}$ and v(C=C)], 1089, 624 [v(ClO$_4^-$)]. LSI–MS, *m/z*: 872 [Cu$_2$L]$^{4+}$. Λ_M/Ω^{-1}cm^{2}mol^{-1} (in CH$_3$CN): 452 (4:1). Color: blue.

2.5.7. [Cd$_2$L](NO$_3$)$_4$·2H$_2$O

Anal. Calc for C$_{46}$H$_{58}$N$_{14}$O$_{14}$Cd$_2$ (MW: 1258.2): C, 43.9; H, 4.6; N, 15.6. Found: C, 43.6; H, 4.5; N, 15.6%. Yield: 45%. IR (KBr, cm^{-1}): 1602, 1575, 1456 [v(C=C) and v(C=N)$_{py}$], 1384, 1095, 821, 771 [v(NO$_3^-$)]. LSI–MS, *m/z*: 1096 [Cd$_2$L(NO$_3$)$_2$]$^{2+}$, 1034 [Cd$_2$L(NO$_3$)]$^{3+}$, 972 [Cd$_2$L]$^{4+}$. Λ_M/Ω^{-1}cm^{2}mol^{-1} (in CH$_3$CN): 280 (2:1). Color: white.

2.5.8. [Cd$_2$L](ClO$_4$)$_4$·3H$_2$O

Anal. Calc. for C$_{46}$H$_{60}$N$_{10}$O$_{19}$Cl$_4$Cd$_2$ (MW: 1424.1): C, 38.8; H, 4.2; N, 9.8. Found: C, 38.7; H, 4.1; N, 9.8%. Yield: 46%. IR (KBr, cm^{-1}): 1602, 1577, 1444 [v(C=N)$_{py}$ and v(C=C)], 1085, 628 [v(ClO$_4^-$)]. LSI–MS, *m/z*: 972 [Cd$_2$L]$^{4+}$. Λ_M/Ω^{-1}cm^{2}mol^{-1}(in CH$_3$CN): 452 (4:1). Color: white.

3. Results and discussion

The ligand L has been synthesized by the N-alkylation of the secondary amines present in the precursor ligand L′ using 2-picolyl chloride hydrochloride in acetonitrile. The macrocycle was characterised by elemental analysis, IR, LSI–MS, ^{1}H and ^{13}C NMR spectroscopy. The IR spectrum shows two splitting bands with maxima at 1589, 1571, 1459, 1434 cm^{-1}, in the region associated with the v(C=N) and v(C=C) vibrations from the pyridine groups, suggesting the incorporation of pyridyl pendant-arms into a pyri-

Table 2
1H and ^{13}C NMR spectra of L in CDCl$_3$.

^{1}H		^{13}C	
Assignment	δ (ppm)	Assignment	δ (ppm)
H$_1$	7.55 (t, 2H)	C$_1$, C$_{10}$	136.2, 135.8
H$_2$, H$_{10}$	7.15 (m, 8H)	C$_2$, C$_9$, C$_{11}$	119.9, 121.6, 122.6
H$_4$	3.95 (m, 4H)	C$_3$, C$_8$	161.5, 161.3
H$_5$	1.25 (s, 12H)	C$_4$	57.9
H$_6$	2.66 (m, 8H)	C$_5$	15.0
H$_7$	3.79 (dd, 8H)	C$_6$	49.8
H$_9$ y H$_{11}$	7.50 (d, 8H)	C$_7$	60.5
H$_{12}$	8.45 (d, 4H)	C$_{12}$	148.7

dine based macrocyclic backbone. The disappearance of the secondary amine stretch at 3300 cm^{-1} in the precursor ligand, L′, further confirms that the alkylation reaction took place. The LSI–MS gave a peak at *m/z* 748 [L+H]$^+$ corresponding to the incorporation of four pyridyl pendant groups in the precursor L′.

The ^{1}H and ^{13}C NMR spectra of L were recorded in CDCl$_3$ solution at 298 K. The proton spectrum (Table 2) shows the expected triplet signal due to the H$_1$ proton of the pyridine units at δ 7.5 ppm, whilst the expected doublet corresponding to H$_2$ collapse in a multiplet at δ 7.1 ppm with the proton signals of the pyridine pendant-arms H$_{10}$. H$_4$ protons appears as a multiplet at δ 3.9 ppm; the methyl groups H$_5$ appears as a singlet at δ 1.2 ppm; the signal at δ 3.8 ppm is attributable to the geminal H$_7$ protons and the aliphatic protons H$_6$ appear as a multiplet at δ 2.6 ppm. (see Scheme 2 for labelling).

The proton spectrum is consistent with an effective C_{2h} symmetry of the 6S,9R,15R,18S-*meso* form of the ligand L found in the crystal structures of the Co(II) and Cd(II) complexes with this ligand. This is confirmed by the ^{13}C NMR spectrum, which shows twelve signals for the 46 carbon nuclei of the ligand backbone. The assignment of the ^{1}H NMR signals was achieved with the aid of standard DEPT, COSY and HMQC experiments (Table 2).
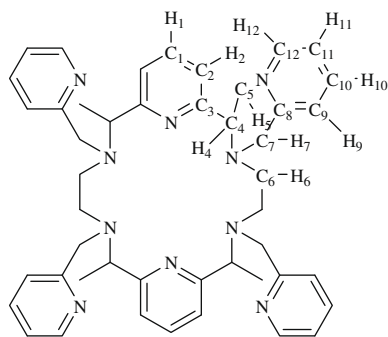
Scheme 2.

The coordination ability of this macrocyclic ligand, L, towards hydrated nitrate and perchlorate salts of Co(II), Ni(II), Cu(II) and Cd(II) was studied. The complexes were synthesized as described in the experimental section and, in general, the reactions gave analytically pure products. Complexes were characterized by microanalysis, LSI–MS, IR, UV–Vis spectroscopy, magnetic studies and conductivity measurements.

The IR spectra of the complexes show similar features. The v(C=N) and v(C=C) bands of the aromatic rings are generally shifted to higher wavenumbers than in the free ligand, suggesting the coordination of the pyridine groups to the metal ions [25].

The IR spectra of the perchlorate complexes feature absorptions attributable to ionic perchlorate at 1100 cm^{-1}. The lack of splitting of this band indicates that these groups are not coordinated to the metal centres [26,27]. Instead, for the nitrate complexes, the band at 1383 cm^{-1} associated with the presence of ionic nitrate is accompanied by several bands in the region associated with nitrate vibrations and these clearly identify the coordinated nitrate groups [28].

The results of LSI–MS of the complexes provide important evidence of the formation of the dinuclear complexes as they feature peaks attributable in all cases to $[M_2L(NO_3)_2]^{2+}$, $[M_2L(NO_3)]^{3+}$ and $[M_2L]^{4+}$ for the nitrate complexes or $[M_2L]^{4+}$ for the perchlorate complexes.

The reflectance spectra of the Co(II) complexes show two d–d transition bands at $ca.$ 10 000 and 20 000 cm^{-1}, which are due to the $^4T_{2g} \leftarrow {}^4T_{1g}$ and $^4T_{1g}(P) \leftarrow {}^4T_{1g}(F)$ transitions, respectively, and are of the type expected for distorted octahedral high-spin Co(II) complexes [29]. The reflectance spectra of the nickel complexes show three bands at $ca.$ 10 300, 16 400 and 26 000 cm^{-1}. These bands are attributable to the $^3T_{2g} \leftarrow {}^3A_{2g}$, $^3T_{1g}(F) \leftarrow {}^3A_{2g}$ and $^3T_{1g}(P) \leftarrow {}^3A_{2g}$ transitions, respectively, and are indicative of octahedral Ni(II) compounds. One absorption band at $ca.$ 14 780 cm^{-1} is also present for nitrate complex, probably due to the spin forbidden transition $^1Eg \leftarrow {}^3A_{2g}$ usually observed in Ni(II) complexes [30,31].

The electronic reflectance spectra of the Cu(II) complexes exhibit a broad band at $ca.$ 17 000 cm^{-1} and an octahedral geometry is proposed [32].

The room temperature magnetic moments obtained for Co(II) complexes (4.6 and 4.7 B.M. per Co atom for nitrate and perchlorate complex, respectively), are consistent with the presence of high-spin octahedral Co(II) ions. The magnetic moments at room temperature for the Ni(II) and Cu(II) complexes were 2.8–2.7 and 1.9–1.8 B.M (per metal atom), respectively, and these values are within the range usually observed for octahedral Ni(II) and d^9 systems, respectively [33].

The molar conductance values for the complexes measured in acetonitrile at 298 K lie in the range reported for 2:1 electrolytes for nitrate and 4:1 for perchlorate complexes [34], showing the different coordinative nature for both type of anions.

3.1. X-ray structures

3.1.1. Crystal structure of [Co$_2$L(CH$_3$CN)$_2$](ClO$_4$)$_4$·2CH$_3$CN

Crystals of [Co$_2$L(CH$_3$CN)$_2$](ClO$_4$)$_4$·2CH$_3$CN adequate to be studied by X-ray diffraction were obtained by slow recrystallization of the complex in acetonitrile. It crystallizes in the monoclinic system, P2(1)/n group. Crystal data and structure refinement are given in Table 1. The molecular structure and selected bond lengths relating to the coordination environment of the metals are given in Fig. 1.

The [Co$_2$L(CH$_3$CN)$_2$](ClO$_4$)$_4$·2CH$_3$CN crystal structure presents a crystallographically imposed symmetry in the unit cell and is consistent with the dinuclear cation complex [Co$_2$L(CH$_3$CN)$_2$]$^{4+}$, four independent perchlorate groups and two crystallization acetonitrile molecules.

The complex structure is endomacrocyclic and each Co(II) ion is coordinated by one pyridyl bridgehead group, the two amine nitrogen atoms contiguous to that pyridyl ring and its corresponding pyridyl pendant-arms. The sixth coordination position is completed by one acetonitrile molecule. Thus, the metal ions are six coordinate with a N$_6$ donor set, and the coordination geometry can be better described as distorted octahedral. The main distortion from a regular geometry can be attributed to the values of the five-membered chelate rings angles at the metal atoms, formed by the tertiary amine and the pyridyl donor groups which deviate significantly from 90°; 73.21(11), 73.47(11), 75.18(11) and 74.72(10)° for N(1)–Co–N(2), N(1)–Co–N(3), N(2)–Co–N(4) and N(3)–Co–N(5), respectively.

The equatorial plane can be considered formed by the nitrogen atoms [N1 N3 N4 N1s (rms 0.6602)]. The Co ion is almost in that plane, displaced only 0.021 Å from them, whilst the axial positions are occupied by the amine N2 and the pyridyl pendant-arm N5 donor atoms [N2–Co–N5, 155.80(11)°].

The structure is quite different to that found previously for [Co$_2$L^1(NO$_3$)$_4$]·2H$_2$O, [Cu$_2$L^1(H$_2$O)$_2$](NO$_3$)$_4$ [17] or [Cu$_2$L^1(CH$_3$CN)$_2$]-(ClO$_4$)$_4$·2CH$_3$CN [15] which consists on a dinuclear exomacrocyclic complexes with the pyridine bridgehead groups non-coordinated to the metal ions.

All the nitrogen donor atoms from the macrocyclic ligand are coordinated to the cobalt ions. The shortest Co–N bond distance corresponds to the pyridyl bridgehead groups, Co–N1, 2.109(3) Å. The Co–N$_{pendant}$ distances are 2.113(3) and 2.168(3) Å, and the
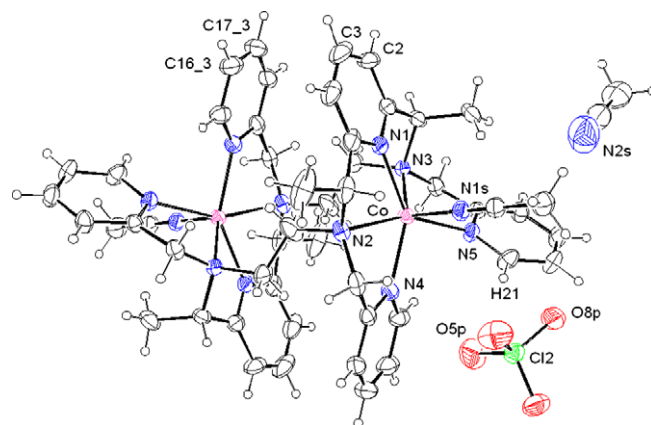

Fig. 1. Crystal structure of [Co$_2$L(CH$_3$CN)$_2$](ClO$_4$)$_4$·2CH$_3$CN complex; selected bond lengths (Å) and angles (°): Co–N(1) 2.109(3); Co–N(4) 2.113(3); Co–N(5) 2.168(3); Co–N(1S) 2.169(3); Co–N(3) 2.312(3); Co–N(2) 2.316(3); N(1)–Co–N(4) 145.89(11); N(1)–Co–N(5) 128.66(11); N(4)–Co–N(5) 84.99(11); N(1)–Co–N(1S) 86.28(11); N(4)–Co–N(1S) 106.00(11); N(5)–Co–N(1S) 82.65(11); N(1)–Co–N(3) 73.47(11); N(4)–Co–N(3) 117.69(10); N(5)–Co–N(3) 74.72(10); N(1S)–Co–N(3) 127.89(11); N(1)–Co–N(2) 73.21(11); N(4)–Co–N(2) 75.18(11); N(5)–Co–N(2) 155.80(11); N(1S)–Co–N(2) 89.52(10); N(3)–Co–N(2) 126.84(10).

Table 3
Shorter atom–atom distances [Å] for $[Co_2L(CH_3CN)_2](ClO_4)_4 \cdot 2CH_3CN$ and $[Cd_2L(NO_3)_2](NO_3)_2 \cdot 2H_2O$.

$[Co_2L(CH_3CN)_2](ClO_4)_4 \cdot 2CH_3CN$		$[Cd_2L(NO_3)_2](NO_3)_2 \cdot 2H_2O$	
C3–C16_$1	3.513(3)	C44–H44···O12n	2.408(3)
C3–C17_$1	3.793(4)	C21–H21b···O9n	2.662(3)
C2–C17_$1	3.645(3)	C20–H20a···O5n	2.369(3)
C21–H21···O5p	2.628(4)	C22–H22c···O2n	2.320(3)
C21–H21···O8p	2.538(3)		

Symmetry transformations used to generate equivalent atoms: $1 $-x + 2$, $-y + 1$, $-z + 1$.

longest coordination bond distances correspond to the amine nitrogen atoms [Co–N2, 2.312(3) Å and Co–N3, 2.316(3) Å]. All of these bond distances are in the order found for similar CoN6 complexes [17,35,36]. Finally, the Co-acetonitrile distance is of 2.169(3) Å, similar to that found in other complexes with a CoN6 core [37,38].

The macrocyclic ligand has a markedly step conformation where the pyridyl bridgehead groups lying parallel to each other, and the angle between these rings and the plane described for the tertiary amine nitrogen atoms (rms = 0) is 89.2(1)°.

The intramolecular Co···Co distance, 5.549 Å, is shorter than that found in $[Co_2L^1(NO_3)_4] \cdot 2H_2O$ (9.33 Å), but too long to consider the existence of a significant intermetallic interaction [39,40].

The pyridyl bridgehead groups (N1C1–C5) and the pyridyl pendant-arms (N4_$1C14_$1–C18_$1) are slightly tilted (dihedral angle 25.7(1)°) with some shorter atom–atom distance (C3–C16_$1, 3.513 Å). However, the centroid–centroid distance of 4.1 Å is too long to suggest the presence of π,π-interactions. Non classical intramolecular H-bonds between non-coordinated perchlorate anions and hydrogen atoms of the pyridine rings (C–H···O) were found (see Table 3).

3.1.2. Crystal structure of $[Cd_2L(NO_3)_2](NO_3)_2 \cdot 2H_2O$

The dinuclear complex $[Cd_2L(NO_3)_2](NO_3)_2 \cdot 2H_2O$ was obtained by recrystallization in acetonitrile of the complex obtained from the reaction between Cd(II) nitrate and the macrocyclic ligand L in a 1:1 molar ratio. The crystal structure was studied by X-ray diffraction and the molecular structure of the complex is shown in Fig. 2 together with the atomic numbering scheme adopted and selected bond length distances (Å) and angles (°).

The $[Cd_2L(NO_3)_2]^{2+}$ cation shows two crystallographically independent cadmium ions located in a similar coordination environment. The metal ions are hexacoordinated and each cadmium ion is surrounded by one pyridyl bridgehead unit, two tertiary amine nitrogens contiguous to that pyridyl bridgehead, and by their corresponding pyridyl pendant-arms. The coordination environment, N_5O core, is completed by a monodentate nitrate anion. The geometry around the metal ions can be described as distorted octahedral, being the equatorial planes that formed by N(1)–N(6)–N(7)–O1n (rms 0.73) and N(3)–N(4)–N(9)–O4n (rms 0.72) for Cd1 and Cd2, respectively. The axial positions are occupied by the amine and pyridyl pendant-arms atoms, N2–Cd1–N10, 161.02(10)° and N5–Cd2–N8, 161.17(10)°.

The crystal structure does not differ to much than that found previously for the dinuclear complexes $[Cd_2L^1(NO_3)_2](NO_3)_2$ [17] and $[Zn_2L^1(NO_3)_2](NO_3)_2 \cdot H_2O$ [19], where the coordinated nitrate anions give rise to a heptacoordinated environment N_5O_2 for cadmium ions, and N_4O pentacoordinated for cinc ions.

The pyridyl bridgehead groups of the macrocyclic backbone provide the shortest bond to the metal atoms [Cd1–N1, 2.274(3) Å, Cd2–N4, 2.267(3) Å]. This distance is slightly shorter than that corresponding to pyridyl pendant-arms [Cd1–N$_{pendant}$, average value of 2.297 Å, and Cd2–N$_{pendant}$, average value of
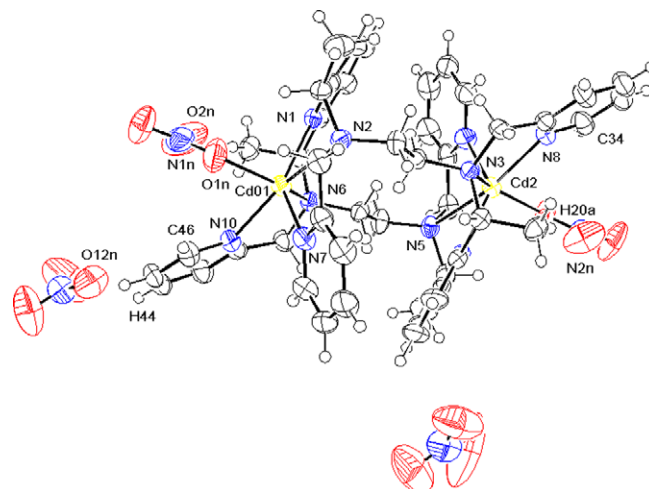

Fig. 2. Crystal structure of $[Cd_2L(NO_3)_2](NO_3)_2 \cdot 2H_2O$ complex; selected bond lengths (Å) and angles (°): N(1)–Cd(01) 2.274(3); N(2)–Cd(01) 2.672(3); N(3)–Cd(2) 2.508(3); N(4)–Cd(2) 2.267(3); N(5)–Cd(2) 2.677(3); N(6)–Cd(01) 2.501(3); N(7)–Cd(01) 2.292(3); N(8)–Cd(2) 2.297(3); N(9)–Cd(2) 2.303(3); N(10)–Cd(01) 2.303(3); O(1 N)–Cd(01) 2.347(3); O(4 N)–Cd(2) 2.330(3); N(1)–Cd(01)–N(7) 134.32(10); N(1)–Cd(01)–N(10) 130.77(10); N(7)–Cd(01)–N(10) 92.56(11); N(7)–Cd(01)–O(1 N) 90.43(13); N(1)–Cd(01)–N(6) 70.97(9); N(7)–Cd(01)–N(6) 119.42(10); N(10)–Cd(01)–N(6) 72.77(10); N(1)–Cd(01)–N(2) 68.20(9); N(7)–Cd(01)–N(2) 69.20(10); N(10)–Cd(01)–N(2) 161.02(10); O(1 N)–Cd(01)–N(2) 85.73(10); N(6)–Cd(01)–N(2) 120.15(9); N(4)–Cd(2)–N(8) 131.21(10); N(4)–Cd(2)–N(9) 133.12(10); N(8)–Cd(2)–O(4 N) 89.97(11); N(4)–Cd(2)–N(3) 71.20(9); N(8)–Cd(2)–N(3) 72.78(10); N(9)–Cd(2)–N(3) 118.36(10); O(4 N)–Cd(2)–N(3) 147.22(10); N(4)–Cd(2)–N(5) 67.58(10); N(8)–Cd(2)–N(5) 161.17(10); N(9)–Cd(2)–N(5) 68.74(10).

2.300 Å], but both types of bonds are quite shorter than those corresponding to the $[Cd_2L^1(NO_3)_2](NO_3)_2$ complex mentioned above. The longest Cd–N bond distance corresponds to the amine groups [Cd1–N$_{amine}$, average value of 2.587 Å and Cd2–N$_{amine}$, average value of 2.642 Å]. Two of the nitrate ions act as monodentate, Cd1–O1n, 2.347(3) Å and Cd2–O4n, 2.330(3) Å, values in accordance with other similar nitrate six coordinated Cd(II) complexes [41–44].

The macrocyclic ligand is also in a step conformation. The dihedral angle between the pyridyl bridgeheads is only of 2(1)° and the angle between these rings and the plane described for the tertiary amine nitrogen atoms (rms 0.0155) is 64.67°.

In this case, the intramolecular Cd···Cd distance is 6.254 Å, longer than the distance found in $[Cd_2L^1(NO_3)_2](NO_3)_2$ (5.784 Å), and also too long to consider the presence of an intermetallic bond.

Non classical intramolecular H-bonds between no coordinated nitrate anions and hydrogen atoms of the pyridine rings and of methyl groups (C–H···O) were also found in the crystal structure (see Table 3).

4. Conclusion

The complexation behaviour of the new tetrapyridyl pendant-armed azamacrocyclic ligand, L, towards nitrate and perchlorate salts of M(II) [M = Co, Ni, Cu, Cd] in acetonitrile have been studied. All the complexes are dinuclear with a distorted octahedral coordination geometry around the metal ions. The crystal structures of $[Co_2L(CH_3CN)_2](ClO_4)_4 \cdot 2CH_3CN$ and $[Cd_2L(NO_3)_2](NO_3)_2 \cdot 2H_2O$ complexes have been determined. In both cases the ligand is bounded to the metal ions by one pyridyl bridgehead group, the two amine nitrogen atoms contiguous to that pyridyl ring and its corresponding pyridyl pendant-arms. The six coordination position is completed by one acetonitrile molecule or by one monodentate nitrate anion. Different non-classical intramolecular H-bonds were found in the crystal structure.

Acknowledgments

Appendix A. Supplementary material

CCDC 738863 and 738864 contain the supplementary crystallographic data for $[Co_2L(CH_3CN)_2](ClO_4)_4 \cdot 2CH_3CN$ and $[Cd_2L(NO_3)_2](NO_3)_2 \cdot 2H_2O$ These data can be obtained free of charge from The Cambridge Crystallographic Data Centre via http://www.ccdc.cam.ac.uk/data_request/cif. Supplementary data associated with this article can be found, in the online version, at doi:10.1016/j.jorganchem.2009.07.013.

References

[1] R.M. Izatt, J.S. Bradshaw, S.A. Nielsen, J.D. Lamb, J.J. Christensen, D. Sen, Chem. Rev. 85 (1985) 271.
[2] K.B. Mertes, J.M. Lehn, in: G. Wilkinson (Ed.), Comprehensive Coordination Chemistry, Pergamon, Oxford, 1987, p. 915.
[3] J.M. Lehn, Angew. Chem., Int. Ed. Engl. 27 (1988) 89.
[4] K.E. Krakowiak, J.S. Bradshaw, D.J. Zamecka-Krakowiak, Chem. Rev. 89 (1989) 929.
[5] J.S. Bradshaw, Aza-Crown Macrocycles, Wiley, New York, 1993.
[6] S.-G. Kang, N.-S. Kim, J.-S. Choi, D. Whang, K. Kim, J. Chem. Soc., Dalton Trans. (1995) 363.
[7] E. Kimura, Y. Kodake, M. Shionya, M. Shiro, Inorg. Chem. 29 (1990) 4991.
[8] K. Hiate, M. Mikuriya, J. Chem. Soc., Dalton Trans. (1990) 2763.
[9] S.-K. Jung, S.-G. Kang, M.P. Suh, Bull. Korean Chem. Soc. 10 (1989) 362.
[10] I.M. Atkinson, J.D. Chartres, G.W. Everett, X.-K. Ji, L.F. Lindoy, O.A. Matthews, G.V. Meehan, B.W. Skelton, G. Wei, A.H. White, J. Chem. Soc., Dalton Trans. (2000) 1191.
[11] P. Xue, Q. Yuan, E. Fu, C. Wu, J. Organomet. Chem. 327 (2001) 637.
[12] W.S. Szulbinski, R.S. Czernuszewicz, Inorg. Chim. Acta 247 (1996) 11.
[13] S.J. Brudenell, L. Spiccia, E.R.T. Tiekink, Inorg. Chem. 35 (1996) 1974.
[14] S.J. Brudenell, L. Spiccia, A.M. Bond, P. Comba, D.C.R. Hockless, Inorg. Chem. 37 (1998) 3705.
[15] R. Bastida, D.E. Fenton, M. López-Deber, A. Macías, L. Valencia, M. Vicente, Inorg. Chim. Acta 355 (2003) 292.
[16] L. Valencia, R. Bastida, A. Macías, M. Vicente, P. Pérez-Lourido, New J. Chem. 29 (2005) 424.
[17] Mª del C. Fernández-Fernández, R. Bastida, A. Macías, L. Valencia, P. Pérez-Lourido, Polyhedron 25 (2006) 783.
[18] Mª del C. Fernández-Fernández, R. Bastida, A. Macías, P. Pérez-Lourido, C. Platas-Iglesias, L. Valencia, Inorg. Chem. 45 (2006) 4484.
[19] L. Valencia, P. Pérez-Lourido, R. Bastida, A. Macías, Crystal Growth Des. 8 (2008) 2080.
[20] Mª del C. Fernandez-Fernandez, R. Bastida, A. Macias, P. Perez-Lourido, L. Valencia, Z. Anorg. Allg. Chem. 633 (2007) 747.
[21] Mª del C. Fernandez-Fernandez, R. Bastida, A. Macias, P. Perez-Lourido, L. Valencia, Polyhedron 26 (2007) 5317.
[22] Mª del C. Fernandez-Fernandez, R. Bastida, A. Macias, P. Perez-Lourido, L. Valencia, Polyhedron 28 (2009) 2371.
[23] G.M. Sheldrick, Sadabs, Program for Empirical Absorption Correction of Area Detector Data, University of Göttingen, Germany, 1996.
[24] SHELXTL Version, An Integrated System for Solving and Refining Crystal Structures from Diffraction Data (Revision 5.1), Bruker AXS Ltd.
[25] N.S. Gill, R.H. Nuttall, D.E. Scaife, D.W. Sharp, J. Inorg. Nucl. Chem. 18 (1961) 3091.
[26] B.J. Hathaway, A.E. Underhill, J. Chem. Soc. (1961) 3091.
[27] P. Guerriero, U. Casellato, S. Tamburini, P.A. Vigato, R. Graziani, Inorg. Chim. Acta 129 (1987) 127.
[28] W.T. Carnall, S. Siegel, J.R. Ferraro, B. Tani, E. Gebert, Inorg. Chem. 12 (1973) 560.
[29] B.P. Lever, Inorganic Electronic Spectroscopy, second ed., Elsevier, Amsterdam, 1984.
[30] W.J. Eilbeck, F. Holmes, A.E. Underhill, J. Chem. Soc. (A) 5 (1967) 757.
[31] J. Reedijk, T.M. Mulder, J.A. Smit, Inorg. Chim. Acta 13 (1975) 219.
[32] B.J. Hataway, R.J. Dudley, P. Nicholls, J. Chem. Soc. (A) (1969) 1845.
[33] B.N. Figgis, Introduction to Ligand Fields, Interscience, New York, 1967.
[34] W.J. Geary, Coord. Chem. Rev. 7 (1971) 81.
[35] L. Valencia, R. Bastida, Mª del C. Fernández-Fernández, A. Macías, M. Vicente, Inorg. Chim. Acta 358 (2005) 2618.
[36] G.R. Newkome, V.K. Majestic, F.R. Fronczek, Inorg. Chim. Acta 77 (1983) L47.
[37] F. Heirtzler, J. Weyhermuller, J. Chem. Soc., Dalton Trans. 3653 (1997).
[38] S. Brooker, R.J. Kelly, P.G. Plieger, Chem. Commun. (1998) 1079.
[39] A. Bondi, J. Phys. Chem. 68 (1964) 441.
[40] C. Janiak, J. Chem. Soc., Dalton Trans. (2000) 3885.
[41] Z. Xu, L.K. Thompson, D.A. Black, C. Ralph, D.O. Miller, M.A. Leech, J.A.K. Howard, J. Chem. Soc., Dalton Trans. (2001) 2042.
[42] R.W. Turner, P.F. Rodesiler, E.L. Amma, Inorg. Chim. Acta 66 (1982) L13.
[43] R.-L. Sang, X. Li, Polyhedron 25 (2006) 2167.
[44] L. Valencia, R. Bastida, A. Macías, P. Pérez-Lourido, Polyhedron 27 (2008) 3509.